

EVOLUTION OF VERY LOW MASS STARS AND BROWN DWARFS. II. THE POPULATION II

FRANCESCA D'ANTONA

Osservatorio Astronomico di Roma; and Istituto di Astrofisica Spaziale C.N.R., Frascati

Received 1986 October 9; accepted 1987 February 25

ABSTRACT

This paper addresses a number of problems connected with the evolution of low-mass ($M \leq 0.8 M_{\odot}$) and very low mass ($M \geq 0.07 M_{\odot}$) stars having metal contents much smaller than the solar metal content, and which are consequently relevant to the understanding of halo and globular cluster low-mass stars. Two main chemical compositions bracketing the Population II regime are considered: helium and metal contents $Y = 0.23$, $Z = 10^{-4}$ (Cox and Stewart opacities) and $Y = 0.25$, $Z = 10^{-3}$ (Alexander, Johnson, and Rypma opacities). For these compositions, the hydrogen burning minimum mass (HBMM) is evaluated. As found by D'Antona and Mazzitelli for Population I, it is confirmed that the atmospheric opacities are the main factor influencing the minimum main-sequence luminosity. In fact, the results show $M_{\min} = 0.11 M_{\odot}$ and $\log(L/L_{\odot}) = -2.93$ ($M_v = 13.5$) for $Z = 10^{-4}$, and $M_{\min} = 0.09 M_{\odot}$, $\log(L/L_{\odot}) = -4.13$ for $Z = 10^{-3}$. As molecular opacities are considered only for the latter chemical composition, the difference between these minimum luminosities must be ascribed not only to the difference in Z , but also to the choice of different opacity sets, and in some ways well represents the uncertainties arising due to the lack of good opacities at low T_{eff} .

Particular care is given to the understanding of the mass luminosity relation. Population II luminosity functions (LFs) are constructed and applied to the interpretation of globular cluster main-sequence LFs. In particular, the low-luminosity end of the main sequence for globular clusters is also predicted.

Subject headings: clusters: globular — luminosity function — opacities — stars: evolution — stars: interiors — stars: Population II

I. INTRODUCTION

In Paper I (D'Antona and Mazzitelli 1985) the evolution of Population I masses $0.8 \geq M/M_{\odot} \geq 0.04$ has been presented, giving particular attention to the influence of atmospheric opacities in predicting the hydrogen-burning minimum mass (HBMM) and the minimum main-sequence luminosity (MMSL). Consideration of molecular and grain opacities (Alexander, Johnson, and Rypma 1983) in fact resulted in a great reduction of the MMSL [$\log(L/L_{\odot}) = -4.35$] with respect to previous computations. Furthermore, at even dimmer luminosities, there appeared to be long-lived structures, down to $M = 0.06 M_{\odot}$, in which nuclear burning and cooling were concomitant sources of energy output for a time comparable to the disk lifetime.

In Paper I, apart from stressing the large uncertainties inherent in the models, due to our poor understanding of grain opacities and to our still incomplete knowledge of the role of H_2O in molecular opacities, we predicted that the reduction of atmospheric opacities, as is the case when considering Population II stars, would have resulted in much larger MMSL. Consequently, it seemed worthwhile to compute the Population II main-sequence limit by adopting the same input physics as in Paper I, in order to provide the first theoretical grounds from which to predict what we must expect from Hubble Space Telescope observations of the lower end of the main sequence in the nearby globular clusters (GCs).

Furthermore, in view of the recent determination of luminosity functions (LFs) for the main sequences of several GCs (McClure *et al.* 1986), the computations have been extended up to $M = 0.75\text{--}0.8 M_{\odot}$, in order to provide the mass luminosity (ML) relations necessary to derive LFs which could be compared with the observations.

As will be shown in § II, there are basic problems in the construction of Population II very low mass star structures. As a result of lowering the metal content, and thus lowering the main donors of opacity, very large densities at the photosphere are obtained. Consequently, the opacities, which until now necessarily have been constructed by inadequate formulations of the equation of state, are inadequate. For these reasons, and considering the present study as an exploratory one, only two representative sets of Population II chemical compositions have been considered, adopting extreme assumptions for their corresponding opacities. Some additional models have been computed for different chemical compositions, in particular lower main-sequence models for zero-metal structures. The results are shown and discussed in §§ IIa and IIb.

Section IIc deals with the consideration and interpretation of the shape of the ML relation up to $0.80 M_{\odot}$ for the two main sets of chemical compositions. In order to compare our models with the observations, we have to adopt bolometric corrections, discussed in § III, which are particularly uncertain at low luminosities. Section III also deals with the LFs constructed adopting several mass functions (MFs). In particular three features of the LF are stressed:

1. There is no gap at $M_v = 7$ corresponding to the so called "Wielen" gap (Wielen 1974) which is present in the field-star LF (Wielen, Jahreiss, and Kruger 1983; discussed in terms of MF by D'Antona and Mazzitelli 1986): it is masked by evolutionary effects.
2. At $M \leq 0.5 M_{\odot}$, the ML relation flattens abruptly, and a sharp rise in the LF is obtained (see also McClure *et al.* 1986), even if a constant MF is adopted.
3. For $M \leq 0.2 M_{\odot}$, the LF must decline, even when considering a still increasing initial mass function (IMF). This is

due to the well-known stretching of the main sequence already discussed in D'Antona and Mazzitelli (1982a, 1983, 1986).

4. In spite of the uncertainties in the bolometric corrections, we guess that, for $M_v \gtrsim 13.5$ there must be *no* stars in the most metal-poor globular clusters, as this is the limiting main-sequence magnitude for $Z = 10^{-4}$.

II. MODEL COMPUTATION AND RESULTS

The evolutionary code (Mazzitelli 1979) and input physics of these computations are the same as in Paper I. Two main sets of models have been computed, corresponding to the following choices of composition and opacities:

1. $Y = 0.23$, $Z = 10^{-4}$, Cox and Stewart (1970) opacities. The mass ranges from 0.8 to 0.1 M_\odot , and all models were evolved through their pre-main-sequence contraction phases, following the procedure described in Mazzitelli and Moretti (1980). Deuterium burning was followed, adopting as the initial deuterium abundance $X_D = 2.5 \times 10^{-5}$.

2. $Y = 0.25$, $Z = 10^{-3}$, opacities interpolated—and extrapolated, when necessary—between the main grid of Alexander, Johnson, and Rypma (1983) and the smaller grids corresponding to lower metal contents. The mass ranges from 0.75 to 0.07 M_\odot . The models down to 0.15 M_\odot were constructed starting from the homogeneous main sequence, whereas for $M \leq 0.12 M_\odot$ the complete evolution from pre-MS was considered, in order to determine accurately the boundary between hydrogen-burning stars and brown dwarfs. A few models starting from pre-MS have been computed for

$Y = 0.23$, $Z = 10^{-3}$ (Alexander, Johnson, and Rypma opacities) to allow comparisons independent of the helium content. The main-sequence location of $M = 0.5 M_\odot$, $Y = 0.23$, $Z = 10^{-3}$ has been computed starting both from the pre-main-sequence and from the homogeneous model. Negligible differences are obtained (mainly in the total He^3 content at a given age), confirming that the two procedures of computation give compatible results.

The MMSL has also been computed for $Y = 0.23$, $Z = 0$ (Cox and Tabor 1976 opacities) by following the evolution of 0.11, 0.115, and 0.12 M_\odot .

The choice of these two main sets of opacities can be justified in the following way: we know that Cox and Stewart (1970) opacities do not include the effects of molecules, whose importance, on the other hand, and with the exception of H_2 , will decrease when the metallicity is reduced. Thus employing Cox and Stewart tables for $Z = 10^{-4}$ means underestimating—but not by too much—the opacity. On the other hand, the Alexander, Johnson, and Rypma (1983) tables *overestimate* the contribution of H_2O , as this opacity is treated by straight-mean method instead of by the opacity sampling technique: thus the opacities employed for $Z = 10^{-3}$ are overestimates. In this way we bracket two somewhat “extreme” chemical compositions for the Population II, and the results should provide some constraints on the information we seek.

As it is highly implausible to find in our Galaxy “young” Population II stars, we present in Figure 1 the H-R diagram of the lower main sequence, and in Tables 1 and 2 relevant data

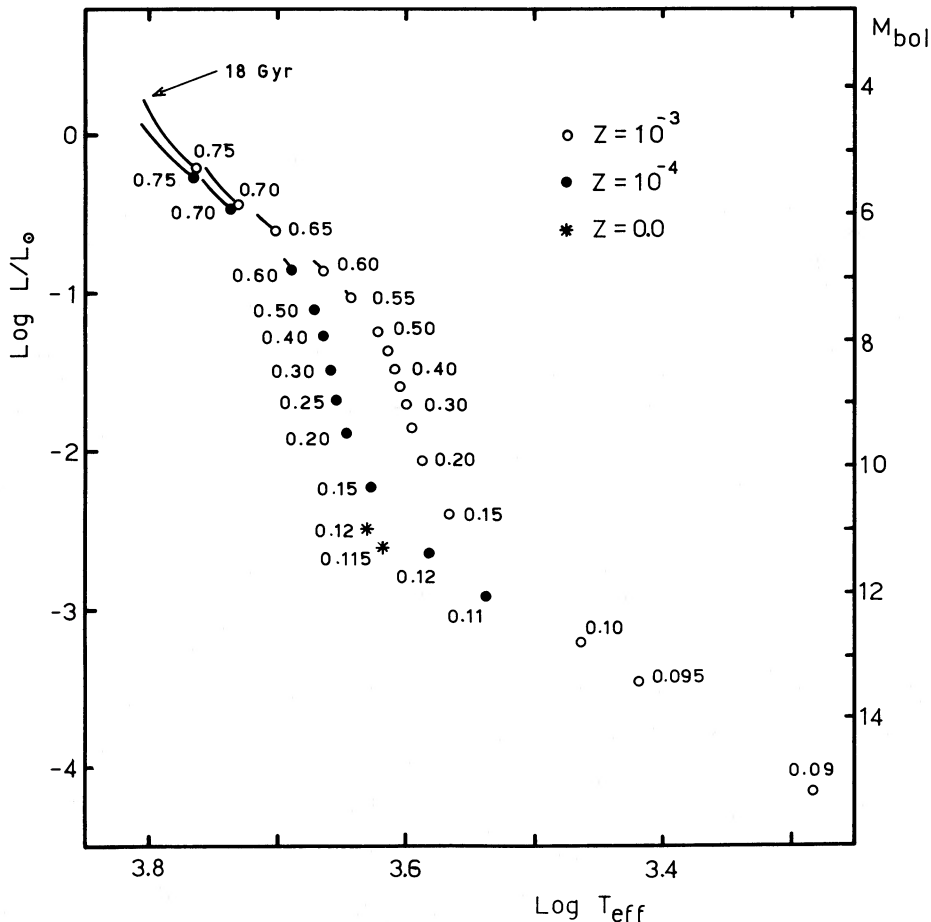


FIG. 1.—H-R diagram of main sequences of computed models. For masses $M \geq 0.55 M_\odot$ the evolution from 10 to 18×10^9 yr (where available) is indicated.

TABLE 1
SELECTED MODELS OF $Y = 0.23, Z = 1.0E - 04$

M/Me	age	logL/L _⊙	LogTe	ξ _c	T _c	X _c	He3	Mce/Me
0.80	1.01e+10	-0.045	3.800	252	1.55e+07	0.215	1.46e-10	0.799
0.80	1.21e+10	0.054	3.812	402	1.70e+07	0.111	"	---
0.80	1.42e+10	0.220	3.826	862	1.98e+07	0.039	"	---
0.75	1.00e+10	-0.263	3.766	176	1.35e+07	0.353	4.12e-10	0.748
0.75	1.20e+10	-0.204	3.774	222	1.44e+07	0.257	"	0.748
0.75	1.50e+10	-0.095	3.789	359	1.59e+07	0.128	"	0.749
0.75	1.81e+10	0.084	3.807	815	1.86e+07	0.041	"	0.749
0.70	1.01e+10	-0.465	3.736	137	1.21e+07	0.461	1.46e-09	0.694
0.70	1.20e+10	-0.430	3.741	159	1.25e+07	0.394	1.46e-09	0.695
0.70	1.49e+10	-0.368	3.749	202	1.33e+07	0.290	"	0.696
0.70	1.82e+10	-0.280	3.760	287	1.45e+07	0.175	"	0.697
0.60	1.04e+10	-0.851	3.691	101	1.02e+07	0.633	1.52e-06	0.549
0.60	1.22e+10	-0.835	3.692	107	1.03e+07	0.592	1.58e-06	0.533
0.60	1.53e+10	-0.809	3.695	119	1.05e+07	0.526	1.64e-06	0.559
0.60	1.82e+10	-0.781	3.697	134	1.08e+07	0.463	1.67e-06	0.565
0.50	1.05e+10	-1.125	3.672	73	8.86e+06	0.729	4.69e-04	0.258
0.50	1.85e+10	-1.120	3.673	87	9.23e+06	0.681	6.56e-04	0.305
0.40	9.77e+09	-1.286	3.666	83	8.00e+06	0.759	5.71e-03	0.000
0.40	1.87e+10	-1.271	3.666	79	7.91e+06	0.753	6.96e-03	0.000
0.30	9.65e+09	-1.518	3.659	126	7.41e+06	0.757	7.77e-03	0.000
0.30	1.65e+10	-1.500	3.659	119	7.32e+06	0.752	9.97e-03	0.000
0.25	1.03e+10	-1.676	3.654	168	7.00e+06	0.756	9.60e-03	0.000
0.25	1.55e+10	-1.660	3.654	160	6.95e+06	0.751	1.19e-02	0.000
0.20	1.01e+10	-1.896	3.647	254	6.48e+06	0.756	1.12e-02	0.000
0.20	1.74e+10	-1.873	3.647	237	6.44e+06	0.749	1.55e-02	0.000
0.15	8.46e+09	-2.242	3.627	467	5.58e+06	0.761	8.60e-03	0.000
0.15	1.46e+10	-2.230	3.628	455	5.60e+06	0.755	1.42e-02	0.000
0.12	1.34e+10	-2.651	3.582	791	4.51e+06	0.763	6.80e-03	0.000
0.11	1.54e+10	-2.954	3.538	986	3.94e+06	0.765	4.53e-03	0.000

TABLE 2
SELECTED MODELS OF $Y = 0.25, Z = 1.0E - 03$

M/Me	age	logL/L _⊙	LogTe	ξ _c	T _c	X _c	He3	Mce/Me
0.75	1.02e+10	-0.209	3.767	206	1.42e+07	0.286	1.98e-14	0.747
0.75	1.21e+10	-0.144	3.776	268	1.51e+07	0.192	"	0.748
0.75	1.32e+10	-0.102	3.781	327	1.57e+07	0.146	"	0.748
0.75	1.80e+10	0.223	3.805	1351	2.12e+07	2.8e-4	6.44e-13	0.749
0.70	1.04e+10	-0.417	3.734	159	1.26e+07	0.393	9.31e-13	0.694
0.70	1.22e+10	-0.378	3.739	185	1.32e+07	0.326	"	0.695
0.70	1.53e+10	-0.300	3.750	248	1.42e+07	0.213	"	0.696
0.70	1.78e+10	-0.221	3.761	354	1.52e+07	0.128	"	0.696
0.65	1.00e+10	-0.631	3.699	124	1.13e+07	0.502	1.17e-04	0.640
0.65	1.50e+10	-0.558	3.710	166	1.21e+07	0.365	5.20e-05	0.641
0.65	1.80e+10	-0.504	3.717	204	1.27e+10	0.281	2.73e-05	0.642
0.60	1.08e+10	-0.833	3.669	110	1.04e+07	0.57	1.37e-08	0.582
0.60	1.45e+10	-0.797	3.673	124	1.07e+07	0.494	1.49e-08	0.584
0.55	1.05e+10	-1.042	3.643	96	9.54e+06	0.651	3.12e-07	0.509
0.55	1.75e+10	-0.995	3.648	114	9.88e+06	0.538	3.77e-07	0.517
0.50	1.00e+00	-1.233	3.624	84	8.85e+06	0.691	1.38e-03	0.416
0.50	1.48e+10	-1.214	3.626	92	9.02e+06	0.660	9.38e-04	0.424
0.50	1.82e+10	-1.200	3.627	98	9.10e+06	0.623	6.36e-04	0.429
0.45	1.06e+10	-1.376	3.614	75	8.30e+06	0.712	9.69e-05	0.277
0.45	1.73e+10	-1.369	3.615	84	8.48e+06	0.684	1.36e-04	0.298
0.40	1.03e+10	-1.485	3.609	74	7.88e+06	0.739	5.24e-03	0.000
0.40	1.75e+10	-1.470	3.609	70	7.79e+06	0.735	6.55e-03	0.000
0.35	1.12e+10	-1.587	3.605	89	7.58e+06	0.738	6.56e-03	0.000
0.35	1.62e+10	-1.577	3.605	86	7.51e+06	0.735	7.71e-03	0.000
0.30	1.05e+10	-1.714	3.601	113	7.28e+06	0.738	7.25e-03	0.000
0.30	1.74e+10	-1.698	3.601	107	7.20e+06	0.734	9.43e-03	0.000
0.25	1.31e+10	-1.863	3.596	146	6.87e+06	0.736	9.53e-03	0.000
0.25	1.84e+10	-1.851	3.596	141	6.83e+06	0.732	1.15e-02	0.000
0.20	1.08e+10	-2.079	3.588	216	6.38e+06	0.738	9.48e-03	0.000
0.20	1.86e+10	-2.061	3.589	206	6.35e+06	0.732	1.36e-02	0.000
0.15	1.14e+10	-2.396	3.571	369	5.52e+05	0.741	8.31e-03	0.000

for the computed evolutions, considering only ages larger than 10 billion yr. We will now discuss several different aspects of the computational results.

a) *Hydrogen-burning Minimum Mass and Luminosity*

The run with time of luminosity and central temperature of the sequences of 0.10, 0.11, 0.12, and 0.15 M_{\odot} of $Z = 10^{-4}$ is shown in Figure 2. The track of 0.11 M_{\odot} reaches the main sequence after 5×10^8 yr, while the 0.10 M_{\odot} sequence always cools down.

Table 3 presents the HBMM data for the three chemical compositions, and, for comparison, the Population I values as given in Paper I. It is easily seen that, while the HBMM varies only by 0.035 M_{\odot} passing from Population I to zero-metal structures, the MMSL varies by about a factor of 60. The largest difference in luminosity, however, is shown by the MMSLs obtained in the present computations for $Z = 10^{-3}$ and $Z = 10^{-4}$, and it is to be ascribed, not only to the change in metallicity, but also to the difference discussed before in the adopted opacities. Keeping in mind that our choice of opacities gives limiting values, the log (L/L_{\odot}) difference in MMSL between 10^{-3} and 10^{-4} should be regarded as the maximum "intrinsic" uncertainty due to our inadequate understanding

TABLE 3

MAIN-SEQUENCE LIMIT AS FUNCTION OF CHEMICAL COMPOSITION

Y	Z	M/M_{\odot}	$\log(L/L_{\odot})$	$\log T_e$	Opacity Tables
0.25.....	0.02	0.080	-4.37	3.195	Alexander <i>et al.</i> 1983
0.25.....	0.001	0.090	-4.13	3.285	Alexander <i>et al.</i> 1983
0.23.....	0.0001	0.110	-2.93	3.540	Cox and Stewart 1970
0.23.....	0.0	0.115	-2.60	3.620	Cox and Tabor 1976

of opacities. For instance, if somewhat smaller opacities for $Z = 10^{-3}$ had been adopted, these would possibly have led to the stabilization of the 0.095 M_{\odot} model, which—at $\log(L/L_{\odot}) = -3.5$ —is brighter than the Population I limit by a factor of 10.

We have to discuss further not only the reliability, but also the availability of opacities: in Figure 3 we show the ρ - T stratification of the models of $Z = 10^{-4}$ close to the HBMM. The 0.11 M_{\odot} main-sequence model is shown, together with two models of 0.10 M_{\odot} . In the first model, at $\log(L/L_{\odot}) = -3.38$, the maximum percentage of nuclear energy generation is reached (68%), while in the second model, at $\log(L/L_{\odot}) = -4.0$, the nuclear energy release produces only 9% of the

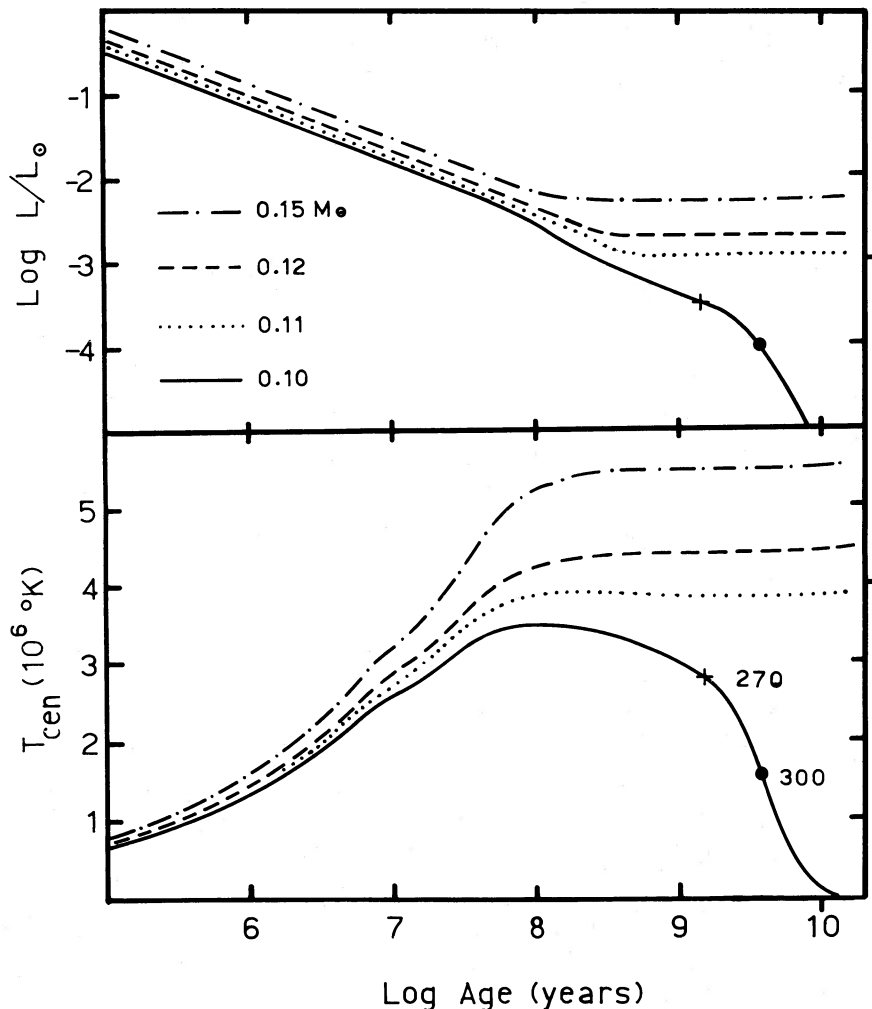


FIG. 2.—Temporal evolution of luminosity and central temperature for 0.10, 0.11, 0.12, and 0.15 M_{\odot} of $Y = 0.23$, $Z = 1.0 \times 10^{-4}$.

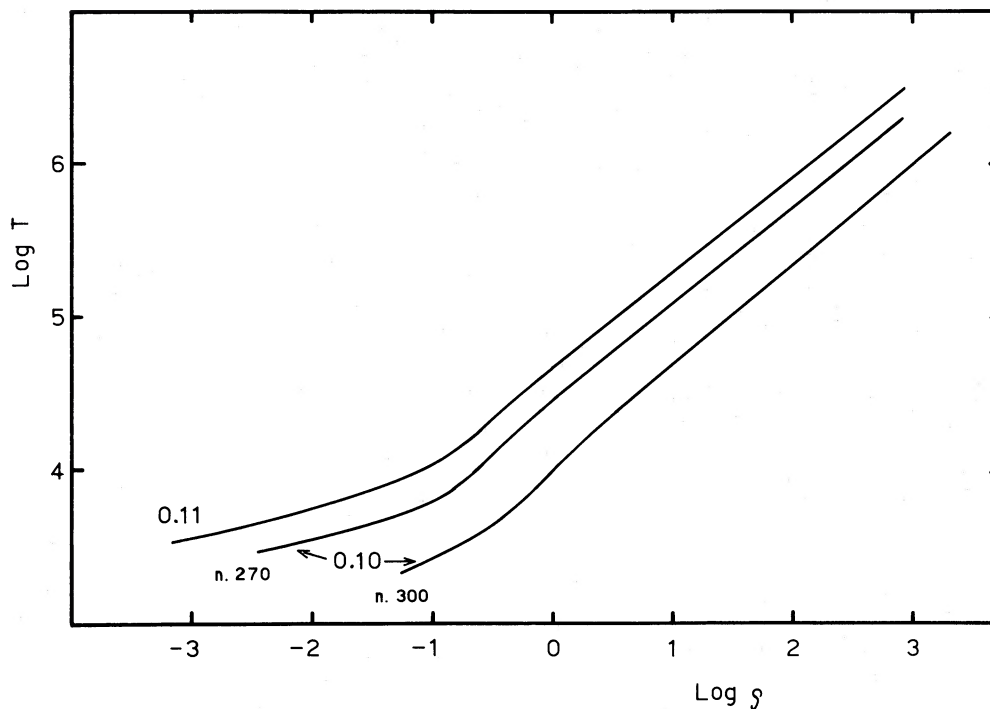


FIG. 3.—Log density vs. log temperature stratification for models of $Z = 1.0 \times 10^{-4}$. At $\log \rho = -0.3$ pressure ionization occurs, and, close to this boundary, covolume pressure largely exceeds corresponding ideal gas pressure (Magni and Mazzitelli 1979; D'Antona and Mazzitelli 1982a). For $M = 0.11 M_{\odot}$ a main-sequence model ($\log [L/L_{\odot}] = -2.93$) is shown. For $M = 0.10 M_{\odot}$, model n.270 has $\log (L/L_{\odot}) = -3.38$, model n.300 has $\log (L/L_{\odot}) = -4.0$.

luminosity. Let us keep in mind that all of these models are fully convective and adiabatic; only the outer atmosphere is radiative, so that the opacity is important only down to the photospheric boundary.

The $0.11 M_{\odot}$ model can still be considered realistic, as the photosphere lies at not unreasonably large densities ($\rho \approx 8 \times 10^{-4} \text{ g cm}^{-3}$). Further, the “destiny” of the $0.10 M_{\odot}$ model is decided at a stage where the predicted structure can be believed with some degree of confidence ($\rho = 3 \times 10^{-3}$), but its following evolution shifts the *photosphere* into the region where the pressure effects on the atomic and molecular levels are dominant, and where the excluded volume effects also must be considered (see Magni and Mazzitelli 1979; D'Antona and Mazzitelli 1982a). In this region, not only is it meaningless to “extrapolate” opacities, but, if opacity computations will ever be performed, a non-ideal-gas equation of state must be used, in view of the strong interactions among molecules. Consequently, while we still regard as realistic the computation of MMSL for $Z = 10^{-4}$, the structure and temporal evolution of Population II brown dwarfs is very uncertain.

Thus we see that the computation of very low mass structures results in a twofold problem:

1. Either we are in the realm of large metal abundance, and, in this case, we must investigate correctly the role of molecules and, further, of grains in determining the opacities (the uncertainty in grain opacity is, in fact, the most crucial factor in the Population I MMSL—see Paper I);

2. Or we are dealing with low-metallicity structures which are hotter and denser so that grains are no longer a problem. But, just because of the reduction in the metals which are the main opacity source, the photospheric region is reached only at densities for which any computations for opacities should

include the relevant nonideal gas effects on the equation of state.

In spite of the uncertainty in the lowest luminosity of the main sequence, we may derive a number of results from our models which can be applied to the interpretation of observational data when these will have become available. In particular, group properties such as the luminosity function of an ensemble of coeval stars do not depend too much on the exact value of the MMSL: what mainly matters is the shape of the ML relation toward the HBMM, and, as for Population I, this relation becomes very steep at the low-mass end (the luminosity varies by a factor of 10 when the mass is reduced by only $0.01 M_{\odot}$). For Population I we have shown (D'Antona and Mazzitelli 1986) that the decline in the LF of field stars is to be ascribed entirely to the steepening of the ML relation in the proximity of the HBMM. It is clear that Population II samples will also demonstrate the same effect, and that this effect will be even more pronounced, as the HBMM is larger in Population II than it is in Population I.

b) The Evolution of Population II Brown Dwarfs

In Tables 4 and 5 we present relevant data for the evolution of brown dwarfs and lowest mass stars having $Y = 0.25$ and $Z = 10^{-3}$. The onset of deuterium burning occurs at an age of $\sim 5 \times 10^5$ yr and lasts for more than 10^6 yr for all the masses considered. The locus of burning occurs at larger luminosities and T_{eff} with respect to the corresponding locus for Population I (compare Table 4 with Fig. 1 of Paper I) but its main characteristics are the same. For instance, deuterium burning provides at maximum 90% of the stellar luminosity, and contraction is never completely halted.

Exhaustion of deuterium is followed by a further contraction

TABLE 4
LOCUS OF DEUTERIUM BURNING FOR $Y = 0.25$, $Z = 1.0E - 03$

M/M_{\odot}	DURATION ($1E + 06$ yr)	LOCUS OF MAXIMUM DEUTERIUM BURNING				
		Age	$\log(L/L_{\odot})$	$\log T_{\text{eff}}$	$\log T_c$	$\log \rho_c$
0.07.....	1.40E + 06	8.86E + 05	-1.225	3.593	5.889	0.314
0.075.....	1.32	8.40	-1.167	3.531	5.896	0.265
0.08.....	1.24	8.26	-1.115	3.533	5.902	0.233
0.085.....	1.20	7.67	-1.064	3.534	5.907	0.179
0.09.....	1.13	7.24	-1.016	3.535	5.912	0.139
0.095.....	1.07	7.22	-0.975	3.536	5.917	0.106
0.10.....	1.03	6.72	-0.932	3.537	5.921	0.069

phase. Around 10^8 yr, all structures reach their maximum central temperature. The total lifetimes at $\log(L/L_{\odot}) > -4.5$ are smaller than 2×10^9 yr for $M < 0.075 M_{\odot}$. The structures at $0.075 \lesssim M/M_{\odot} \lesssim 0.085$ can be considered the equivalent of Population I transition masses, as they live for several billion yr at $-4.5 \lesssim \log(L/L_{\odot}) \lesssim -4.0$.

We have already discussed that the uncertainty in the opacities does not allow the definitive determination of $M = 0.09 M_{\odot}$ as HBMM for this chemical composition.

TABLE 5
EVOLUTION OF BROWN DWARFS $Y = 0.25$, $Z = 1.0E - 03$

log age	logL/L _o	logTeff	logTc	log ρ_c	phase
M=0.07M_o					
7.0015	-2.045	3.5424	6.248	1.592	contraction
7.9778	-2.855	3.499	6.393	2.465	max Tc
8.0032	-2.879	3.496	6.393	2.482	
9.0026	-4.102	3.270	6.227	2.938	
9.2532	-4.517	3.176	6.157	2.995	
M=0.075M_o					
7.0026	-2.001	3.545	6.268	1.577	contraction
8.0015	-2.808	3.508	6.426	2.474	max Tc
9.0076	-3.976	3.302	6.286	2.980	Lnuc=2%
9.3394	-4.502	3.184	6.194	3.057	Lnuc=16%
M=0.08M_o					
7.0021	-1.959	3.548	6.286	1.562	contraction
8.0016	-2.747	3.517	6.456	2.466	Lnuc=20%
8.0745	-2.812	3.511	6.456	2.517	max Tc
9.0003	-3.832	3.337	6.350	3.003	
9.5005	-4.553	3.176	6.218	3.118	Lnuc=36%
M=0.085M_o					
7.0026	-1.921	3.551	6.304	1.549	contraction
8.0014	-2.692	3.526	6.482	2.459	
8.1467	-2.819	3.513	6.484	2.560	max Tc
9.0063	-3.696	3.369	6.406	3.013	Lnuc=38%
9.7775	-4.578	3.175	6.244	3.173	Lnuc=75%
M=0.09M_o					
7.0030	-1.885	3.553	6.319	1.531	contraction
8.0030	-2.643	3.532	6.506	2.452	
8.2165	-2.825	3.515	6.511	2.603	max Tc
9.0090	-3.540	3.402	6.461	3.004	Lnuc=60%
10.0265	-4.087	3.292	6.360	3.163	Lnuc=96%
10.1938	-4.135	3.281	6.351	3.172	
M=0.095M_o					
7.0021	-1.851	3.555	6.333	1.513	contraction
8.0000	-2.594	3.539	6.528	2.442	Lnuc=75%
8.2621	-2.810	3.519	6.537	2.629	max Tc
9.0034	-3.336	3.437	6.510	2.976	
9.7573	-3.461	3.420	6.501	3.018	Lnuc=100%
10.2277	-3.454	3.422	6.503	3.017	
M=0.10M_o					
7.0012	-1.817	3.557	6.345	1.495	contraction
8.0067	-2.556	3.543	6.549	2.439	
8.3938	-2.862	3.516	6.562	2.709	max Tc
9.0088	-3.199	3.468	6.552	2.935	Lnuc=92%
9.6019	-3.223	3.464	6.551	2.950	Lnuc=100%
10.0931	-3.2174	3.465	6.553	2.948	

c) *The Shape of the Mass Luminosity Relation at $0.3 < M/M_{\odot} < 0.8$*

A complete consideration of the LF of coeval stars of low metallicity also requires knowledge of the ML relation for larger masses, as, in any case, the number counts in different magnitude intervals must be normalized to some "safe" reference count at a brighter magnitude. In practice, it is necessary to compute models for the masses up to the masses which, at an age ranging from 12 to 18 billion yr, are already evolving. The theoretical ML relations for the two sets of chemical composition are shown in Figure 4 at a representative age of 15×10^9 yr, and are compared with the relation for Population I taken from the models of Paper I and from unpublished main-sequence models by Mazzitelli for $M \geq 0.6 M_{\odot}$ at an age of 10^9 yr. Thus, the comparison shows the main differences to be taken into account when dealing with Population I or II. These are as follows:

1. The age effect: Population I stars have a distribution of ages. In particular, the age of Population I stars of $M \geq 1 M_{\odot}$ which are still in main sequence must be smaller than their proper evolutionary time off the main sequence. On the contrary, Population II star samples are constrained in age by the fact that they have all been formed on a short time interval, an interval of the order of the galaxy disk formation time for halo stars, and probably an even shorter interval for globular cluster stars. Consequently, the quantity dM/dL , which enters as a crucial factor in the determination of the LF for stars that evolve significantly in times which are shorter than the galactic age, becomes very small, until it is practically zero at the mass, determined by age and chemical composition, which now populates the giant region in a given sample.

2. Conversely, the Population II ML relation at the low-mass end is steeper than it is in Population I, due to the combined effects of increasing the HBMM when reducing the metallicity and of not needing to consider the brown dwarf cooling tracks, as all brown dwarfs have cooling times much shorter than the galactic age.

3. Both in Population I and II, the derivative of the ML relation increases at $0.4 \lesssim M/M_{\odot} \lesssim 0.55$, the exact value depending on Z . In the range $0.4 \lesssim M/M_{\odot} \lesssim 0.2$, as the metal abundance becomes less, the stellar luminosity becomes larger, reaching a difference of about a factor of 3 at $M = 0.3 M_{\odot}$, between the $Z = 10^{-3}$ and the $Z = 10^{-4}$ models.

The theoretical reasons for this behavior must be carefully traced. Two facts are concomitant with this bifurcation of the ML relation: first, the He^3 equilibrium in the p - p burning chain is no longer reached at $M \leq 0.5 M_{\odot}$, even for an age of 15 billion yr; second, external convection deepens into the star, until, at $M = 0.4 M_{\odot}$, it meets the inner convective core, and the structure becomes fully convective. As the internal struc-

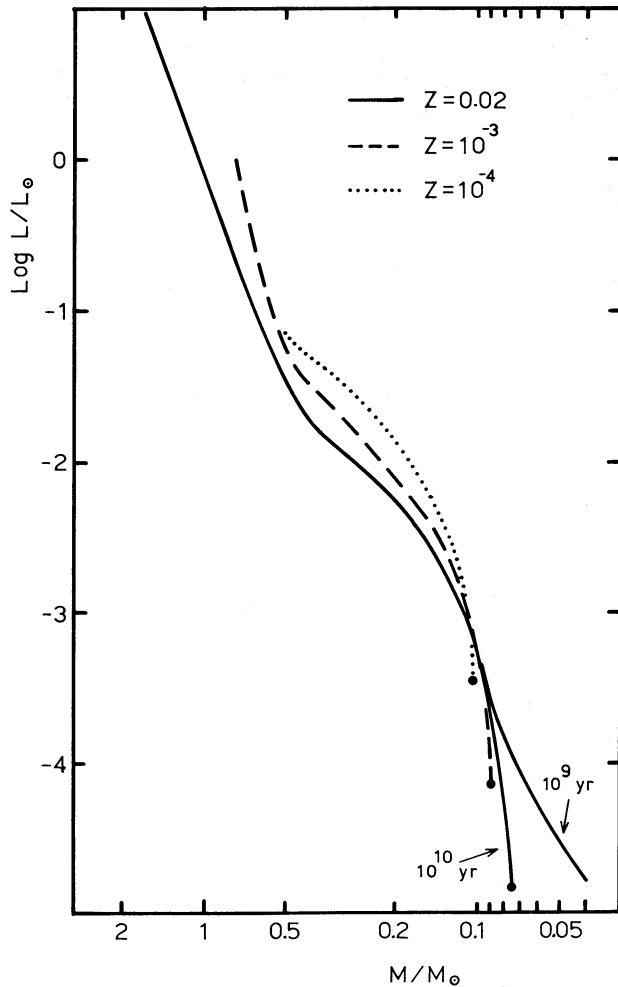


FIG. 4.—Theoretical mass-luminosity relations for Population II, at 15×10^9 yr, compared to those of Population I (D'Antona and Mazzitelli 1985, 1986). Models of $M > 0.6 M_{\odot}$ refer to main-sequence ages, and two lines at $M < 0.1$ refer to 10^9 yr and 10^{10} yr. Points indicate HBMM.

ture is not very dependent on the metal content, the energy production by p - p burning is about the same for $Z = 10^{-4}$ and $Z = 10^{-3}$. When the structure becomes fully convective, the luminosity output is dependent directly on the opacity of the surface layers; thus, a comparable production of nuclear energy results in structures of larger luminosity, as Z decreases. The nonequilibrium of He^3 is globally less important, although the model luminosities slowly increase with age, following the increase of He^3 in the core (see also Neece 1984 for a discussion).

III. OBSERVATIONAL CONSEQUENCES: THE LUMINOSITY FUNCTION

Computation of the observational LFs first of all requires conversion of the theoretical data into observed quantities. As, at present, the visual magnitude is the most widely used observable quantity for globular clusters photometry, it is necessary to know adequate bolometric corrections. For Population I this step is straightforward, as we may adopt semiempirical correlations $M_{\text{bol}} - M_v$ (see Lacy 1977), avoiding use of the theoretical T_{eff} , which may be systematically biased (it is well-known that radii of low-mass stars are generally underestimated by the theoretical models). In this case, there are not

enough data for semiempirical calibrations so that the more uncertain procedure must be adopted. Remember, however, that we do not pretend to present definitive results but mainly indications of the LF's global behavior.

We convert the $\log(L/L_{\odot})$ into M_v by adopting the bolometric corrections by Vandenberg and Bell (1985) from 7000 to 4500 K. At lower T_{eff} we link their results for metallicity $[M/H] = -1$ ($Z = 0.0017$) to the results by Mould and Hyland (1976), available at $T_{\text{eff}} < 4170$ K. Vandenberg and Bell (1985) BCs are available also for metallicities reduced down to $[M/H] = -3$ ($Z = 1.7 \times 10^{-5}$), and these have been extrapolated to smaller T_{eff} , using the Mould and Hyland calibration as a reference line.

In Figure 5 we present the $M_v - M/M_{\odot}$ relation for $Z = 10^{-4}$ (age 15×10^9 yr), for $Z = 10^{-3}$ (ages 12, 15, and 18×10^9 yr), and the relation adopted for Population I in D'Antona and Mazzitelli 1986. This comparison shows, even more emphatically than does the theoretical comparison, the difference between the populations. The remarkable change in dM_v/dM which is apparent in Population II at $M \lesssim 0.5 M_{\odot}$ appears much smoother in Population I (as the age effect is not present). In Population I, an inflection in the dM_v/dM appears around $M_v = 7$, and produces a dip in the LF of field stars (Wielen 1974), even if the mass function is monotonic (Mazzitelli 1972; D'Antona and Mazzitelli 1986). This behavior is masked, in Population II, by the evolutionary (age) effects, so that we *do not* expect a dip in the LF of Population II stars.

The next step follows easily: the LF is obtained by assuming a given shape for the actual mass function (MF) of the considered sample, and the ML relation at a given age:

$$\varphi = dN/dM_v = (dN/dM)/(dM/dM_v),$$

$$M = M(M_v, t).$$

As generally used, we assume:

$$dN/dM = KM^{-(1+x)},$$

and plot in the figures the quantity $\log_{10}(\varphi)$.

Figure 6 shows the LFs obtained by assuming $x = 1$ and ages 12, 15, and 18×10^9 yr for the two metallicities. The curves of each Z are normalized in order to coincide at magnitudes where the age effect is negligible. This requires an assumed M_v (normalization) > 6.25 ; for $M_v < 6$ ($Z = 10^{-3}$) or $M_v < 5.75$ ($Z = 10^{-4}$) different ages spread the LFs.

Three features appear to be dominant in the shape of this LF:

1. A sharp rise at $M_v = 7$ ($Z = 10^{-4}$) or $M_v = 8.5$ ($Z = 10^{-3}$). It is *only* a function of metallicity, and will be present with *any* shape of the MF. This result is shown in Figure 7, where the LFs are plotted for age = 15×10^9 yr and for several values of x . Even with a flat MF we expect an increase by a factor of at least 2 in the LF passing from $M_v = 7$ (or 8, according to the metallicity) to $M_v = 9$. We may add that our sequences probably bracket these "turn up" magnitudes for most of low-metallicity GCs, as the $Z = 10^{-4}$ opacities are underestimates (no molecules in Cox and Stewart opacities), while the $Z = 10^{-3}$ opacities are overestimates (because of water vapor opacity).

2. Even if the MF has a steep slope ($x = 1$ or 1.5) we must expect a plateau below $M_v = 9$, which, for $Z = 10^{-4}$, extends to $M_v = 13$. This corresponds to the plateau in the observa-

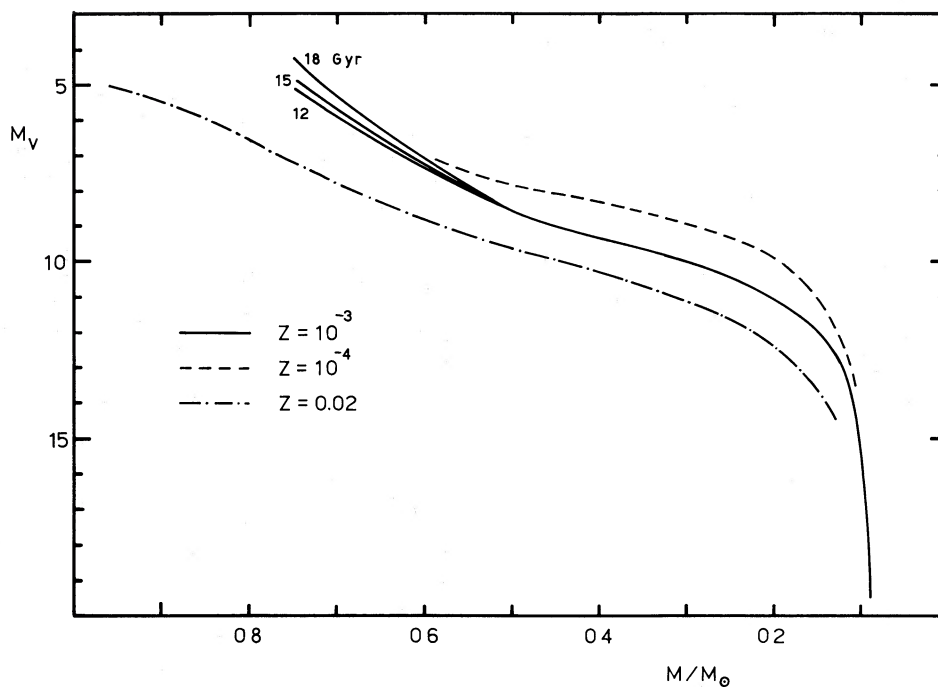


FIG. 5.—Mass-visual magnitude relation for Population I (D'Antona and Mazzitelli 1986), for $Y = 0.23$, $Z = 10^{-4}$, at 15×10^9 yr, and for $Y = 0.25$, $Z = 10^{-3}$, at 12, 15, and 18×10^9 yr.

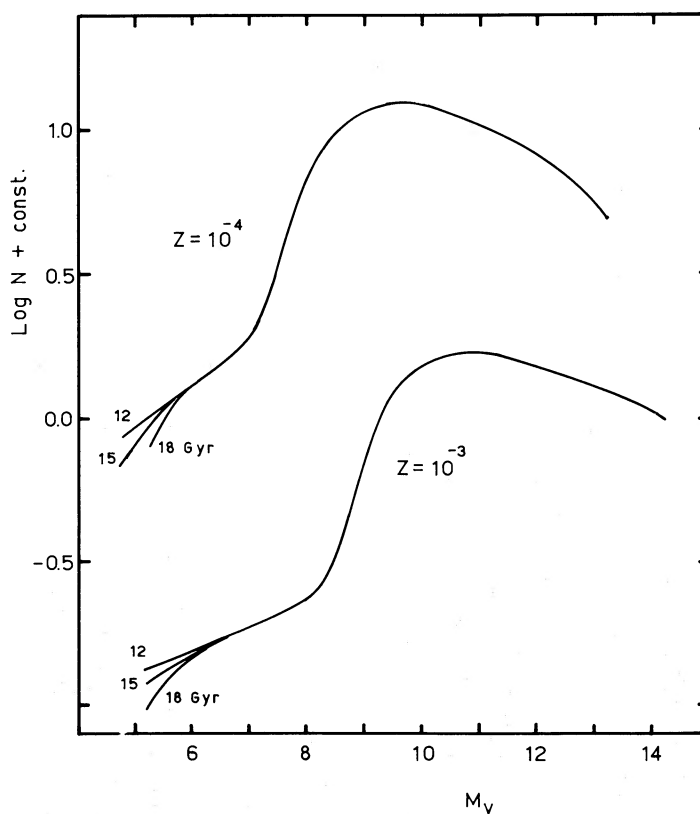


FIG. 6.—Luminosity functions for the two chemical compositions, at 12, 15, and 18×10^9 yr, adopting a mass function of index $x = 1$. Normalization set at $M_v = 6.25$.

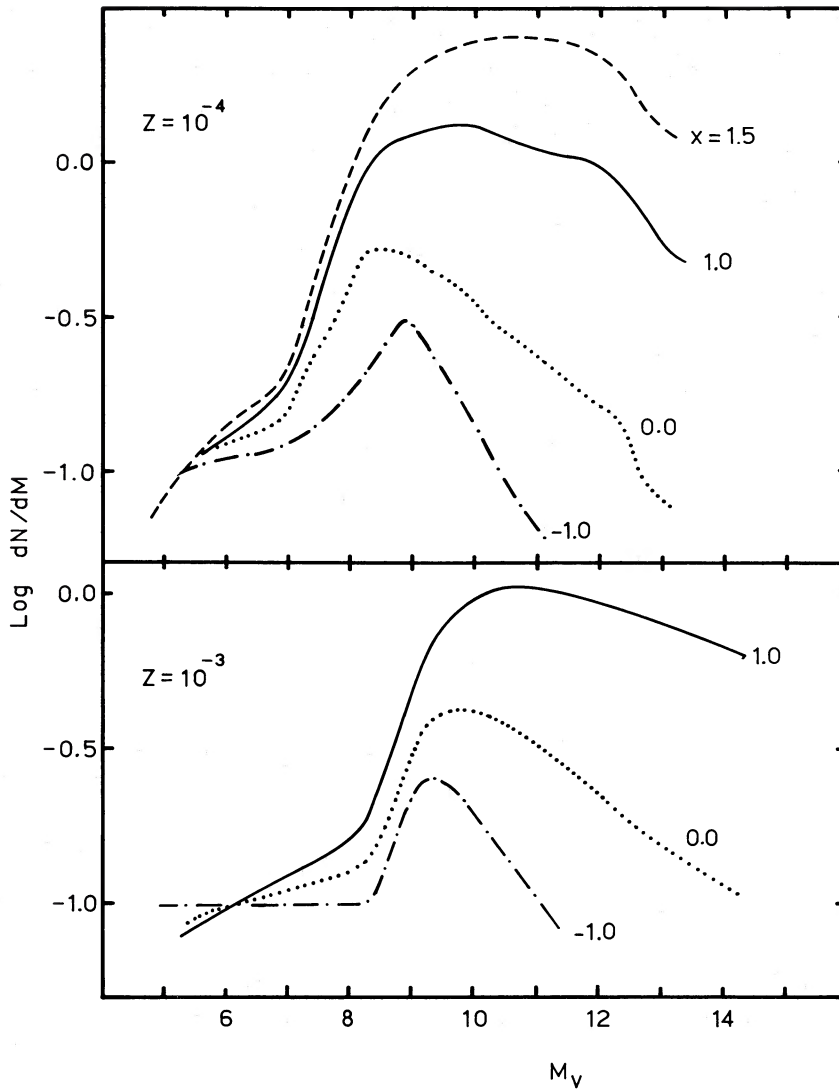


FIG. 7.—Luminosity functions at 15×10^9 yr for several values of mass function index. Normalization of the $Z = 10^{-4}$ LFs (upper) is made at $M_v = 5.25$. Normalization for $Z = 10^{-3}$ (lower) is at $M_v = 6.25$.

tional LF of Population I stars, and is due to the steepening of the ML relation at $M \lesssim 0.2 M_{\odot}$ (this feature has been widely discussed in D'Antona and Mazzitelli 1983, 1986).

3. If our determination of the HBMM is correct, *no stars* should have $M_v > 13.5$ in the lowest metallicity globular clusters, while the MS can extend to dimmer magnitudes in more metal-rich clusters. This could be the most interesting feature to be checked by HST observations.

IV. COMPARISONS WITH OBSERVATIONS

The theoretical LF of GC main sequences has recently been considered by McClure *et al.* (1986), whose results are qualitatively in agreement with the present ones: mainly, both studies predict that, with increasing metallicity, the M_v at which the sharp rise in the LF must be present becomes dimmer. A quantitative comparison with McClure *et al.* (1986) LFs is made difficult by the fact that they plot the LF itself, in place of its logarithm, and normalize at a point ($M_v = 5.25$) where there is still a dependence of the LF on the adopted age (see Fig. 6). Obviously, the logarithm choice of representation is more

immediate for the comparisons, as any normalization corresponds to a simple shift of the ordinate scale.

In Figure 8 the theoretical LFs for $Z = 10^{-4}$, $x = 1.5$, ages 15 and 18×10^9 yr, are compared with the LF by McClure *et al.* (1986) which refers to an age of 16×10^9 yr and to the same metallicity and slope. The two LFs correspond quite well in the evolutionary part, but the latter point computed by McClure *et al.* is ~ 0.3 dex lower than is ours. It is difficult to trace the origin of this discrepancy, which, if real, would appear more clearly in the dimmer part of the LF; small differences in the mass-luminosity relation or even in the adopted bolometric corrections may give origin to such a difference quite easily. Probably this comparison shows the intrinsic uncertainty in the derivation of the slope of the IMF in this magnitude regime. A further complication arises when comparisons with observed LFs are attempted; in the central part of Figure 8 are plotted the M15 LF data, taken by McClure *et al.* (1986), the theoretical LFs of age 15×10^9 yr, $Z = 10^{-4}$, and three different slopes of the IMF. It is clear that, while the $x = 1$ IMF probably represents better the whole shape of the LF, the

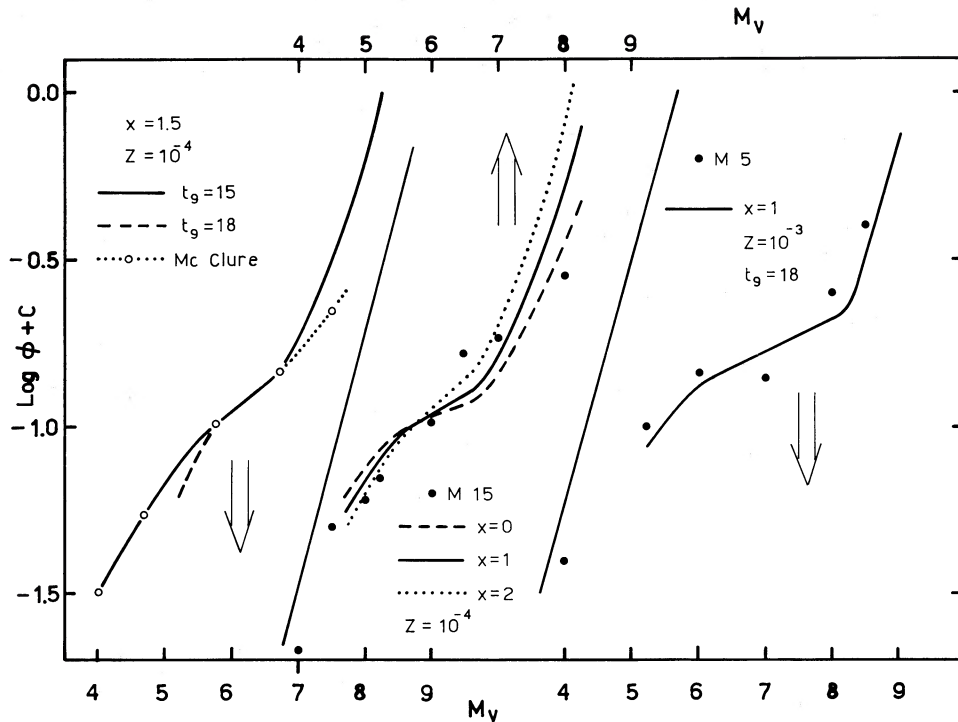


FIG. 8.—Left part of figure presents comparison between theoretical LFs for $x = 1.5$, $Z = 10^{-4}$, ages 15 and 18×10^9 yr, and LF by McClure *et al.* (1986) for same x and Z , but for age 16×10^9 yr. In central and right part, observational LFs for clusters M15 and M5 (data from McClure *et al.* 1986) are compared with theoretical curves.

$x = 2$ or $x = 0$ IMFs must be either considered or discarded, depending on the significance to be placed on the point at $M_v = 8$. From Figure 6, however, it appears that it would be sufficient to gain another magnitude in the photometry to reach the plateau region of the LF, and determine the slope of the IMF more accurately. For now, it is difficult to see whether the trend of variation in slope with metallicity found by McClure *et al.* really exists, at least at the low-metallicity end. For instance, the M5 data by McClure *et al.* can be reasonably fitted by the present models of $Z = 10^{-3}$ and $x = 1$ (see the right part of Fig. 8), so that the same x can be adopted both for the very metal-poor cluster M15 and for a relatively more metal-rich cluster like M5. This lack of a strict correlation between x and Z at the low Z values is also confirmed by another recent analysis by McClure *et al.* (1987). The present study does not deal, however, with the most metal-rich compositions, for which the possibility of a lower slope of the IMF is left open. For instance, the cluster 47 Tuc must be interpreted by data sets referring to metallicity much larger than $Z = 10^{-3}$ (e.g., Gratton, Quarta, and Ortolani 1986).

As a conclusion, while present-day quantitative comparisons

between theoretical LFs and observations of GCs are still subject to large indeterminations, deeper photometry of the nearby GCs could provide, in the near future, much more accurate values for the index of the IMF, by comparison with the level of the peak of the observed and theoretical LFs.

HST observations could further be able to obtain photometry down to the MMSL, which, for the most metal-poor clusters, is predicted to be as small as $M_p = 13.5$.

It is a pleasure for me to thank the Istituto di Astrofisica Spaziale of C. N. R., Frascati for allowing the use of the computer time necessary for the present computations. Italo Mazzitelli is thanked for providing the evolutionary code, and for his always generous help. Discussions on the subject of globular clusters with Vittoria Caloi and Raffaele Gratton, and discussion on the shape of the globular cluster luminosity function with Harvey Richer and Alvio Renzini have stimulated the completion of this work. An anonymous referee provided useful suggestions for a more complete and better presentation of this paper.

REFERENCES

- Alexander, D. R., Johnson, H. R., and Rypma, R. L. 1983, *Ap. J.*, **272**, 773.
 Cox, A. N., and Stewart, J. N. 1970, *Ap. J. Suppl.*, **19**, 243.
 Cox, A. N., and Tabor, T. E. 1976, *Ap. J. Suppl.*, **31**, 271.
 D'Antona, F., and Mazzitelli, I. 1982a, *Astr. Ap.*, **113**, 303.
 ———. 1982b, *Ap. J.*, **260**, 722.
 ———. 1983, *Astr. Ap.*, **127**, 149.
 ———. 1985, *Ap. J.*, **296**, 502 (Paper I).
 ———. 1986, *Astr. Ap.*, **162**, 80.
 Gratton, R. G., Quarta, M. L., and Ortolani, S. 1986, *Astr. Ap.*, **169**, 208.
 Lacy, C. H. 1977, *Ap. J. Suppl.*, **34**, 479.
 Magni, G., and Mazzitelli, I. 1979, *Astr. Ap.*, **72**, 134.
 Mazzitelli, I. 1972, *Ap. Space Sci.*, **17**, 378.
 ———. 1979, *Astr. Ap.*, **79**, 251.
 Mazzitelli, I. and Moretti, M. 1980, *Ap. J.*, **235**, 955.
 McClure, R. D., *et al.* 1986, *Ap. J. (Letters)*, **307**, L49.
 McClure, R. D., *et al.* 1987, in *IAU Symposium 126, Globular Cluster Systems in Galaxies*, ed. J. Grindley and A. G. Davis Philip: (Dordrecht: Reidel), in press.
 Mould, J. R., and Hyland, A. R. 1976, *Ap. J.*, **208**, 399.
 Neece, G. D. 1984, *Ap. J.*, **277**, 738.
 Vandenberg, D. A., and Bell, R. A. 1985, *Ap. J. Suppl.*, **58**, 561.
 Wielen, R. 1974, in *Highlights of Astronomy*, Vol. 3, ed. G. Contopoulos (Dordrecht: Reidel), p. 395.
 Wielen, R., Jahreiss, H., and Kruger, R. 1983, in *IAU Colloquium 76 The Nearby Stars and the Stellar Luminosity Function*, ed. A. G. Davis Philip and A. R. Uggren (Schenectady: Davis), p. 155.